INTERNATIONAL FIRE DETECTION RESEARCH PROJECT

Field Modeling:
Simulating the Effect of Sloped Beamed Ceilings
on Detector and Sprinkler Response

TECHNICAL REPORT
Year 2

Prepared by

William D. Davis, Ph.D.
Glenn P. Forney, Ph.D.
Richard W. Bukowski, P.E.
Building & Fire Research Laboratory
National Institute of Standards & Technology

NATIONAL
FIRE PROTECTION
RESEARCH FOUNDATION

FIRE RESEARCH

Foreword

The International Fire Detection Research Project was initiated in 1990 with the overall aim of improving fire detection and reducing field installation problems. The ultimate goal of this research project is to increase the reliability of placement of heat and smoke sensing systems in spaces with complex ceiling geometries and high ventilation rates.

This technical report documents results from the second year's application of three-dimensional field modeling to ceiling slopes of 10, 25 and 50 degrees, with beams running along or across the slope. It was found that channeling of smoke flow was more prevalent as ceiling slope increased for parallel beam cases. For beams perpendicular to the slope, increasing the ceiling slope decreased the effectiveness of the beams in preventing smoke flow up the ceiling. The first year's technical report deals with flat ceilings.

The first phase of the project resulted in a Literature Review and Technical Analysis, a comprehensive international survey of the literature on fire detection in a variety of subject areas, with suggestions for future research to fill in some of the gaps in the data. A full technical report on the results is available from the Foundation.

The Research Foundation expresses its gratitude to NIST's Building and Fire Research Laboratory's research team leader, Richard W. Bukowski, P.E., and the authors, for their ground-breaking work using sophisticated 3-dimensional field modeling techniques. And the Foundation also wishes to thank Industrial Risk Insurers for their special assistance with the production of this report.

The Foundation and the authors wish to thank the project's sponsors, the Fire Detection Institute and Technical Advisory Committee listed on the next page for their contributions of expertise, and the financial resources required to complete the second of the four years of research. Opinions expressed here are those of the authors. Of course, sponsorship does not necessarily constitute a sponsor's agreement with every statement in this report.

INTERNATIONAL FIRE DETECTION RESEARCH PROJECT
Three Dimensional Field Modeling for Fire Protection

TECHNICAL ADVISORY COMMITTEE

Allied-Signal Aerospace Co./U.S. Department of Energy
Automatic Fire Alarm Association
Bellcore
Building Officials & Code Administrators
Canadian Fire Alarm Association
Carmel-by-the-Sea, CA Fire Marshal
Cerberus Technologies
Edwards Systems Technology
Environment One
Electric Power Research Institute
Fire Detection Institute
IEI/Vesda
Industrial Risk Insurers
International Conference of Building Officials
International Fire Code Institute
Liberty Mutual Insurance Company
National Burglar & Fire Alarm Association, Inc.
National Electrical Manufacturers Association
National Institute of Standards & Technology
NFPA Technical Committee on Automatic Sprinklers
North Carolina Department of Insurance
Rolf Jensen & Associates
SFPE Educational and Scientific Foundation
Simplex Time Recorder Co.
Southern Building Code Congress, International
System Sensor & Firelite/Notifier
Underwriters Laboratories Inc.
U.S. Fire Administration
U.S. General Services Administration

Contents

List of Figures

List of Tables

Simulating the Effect of Sloped Beamed Ceilings on Detector and Sprinkler Response

William D. Davis   Glenn P. Forney   Richard W. Bukowski

Abstract

The rapid activation of fire detection and suppression systems in response to a growing fire is one of the important factors required to provide for life safety and property protection. Rapid activation requires that sensors be located at optimal distances both beneath the ceiling and radially from the fire. Ceiling obstructions, such as beams and joists, and ceiling slope can significantly modify the flow of smoke along the ceiling and must be taken into consideration when a particular detection system is designed. At present, the standards used to guide the design of these systems contain very little quantitative information concerning the impact of beamed, sloped ceilings on sensor placement.

A multiyear, International Fire Detection Research Project sponsored by the National Fire Protection Research Foundation (NFPRF) was initiated to provide quantitative information on the impact of beams, ceiling slope, and forced ventilation on the movement of smoke in commercial/Industrial properties. During the first year of the project, numerical modeling was validated and additional simulations of level, beamed ceilings for detection of growing fires at design fire sizes of 100 kW and 1 MW were completed. It was found that conditions under beams may be equivalent in some cases to conditions in the channels between the beams at an equivalent height beneath the beam or ceiling respectively. Also, depending on detectable fire size, beam depth and beam spacing, smoke detectors or quick response fusible links may not be necessary for each beam channel.

This report describes the results of the second year of the project. During the second year, numerical simulations of smoke movement in response to sloped, beamed ceilings were studied. Slopes of 10, 25 and 50 degrees were studied with beams running along or across the slope. It was found that channeling of smoke flow was more prevalent as ceiling slope increased for parallel beam cases. For beams perpendicular to the slope, increasing the ceiling slope decreased the effectiveness of the beams in preventing smoke flow up the ceiling. Based on the predicted smoke movement, recommendations on sensor selection and placement are made for sloped, beamed ceilings.

1   Introduction

The rapid activation of fire detection and suppression systems in response to a growing fire is one of the important factors required to provide for life safety and property protection. Rapid activation requires that sensors be located at optimal distances both beneath the ceiling and radially from the fire. Ceiling obstructions, such as beams and joists, and ceiling slope can significantly modify the flow of smoke along the ceiling and must be taken into consideration when a particular detection system is designed. At present, the standards used to guide the design of these systems contain very little quantitative information concerning the impact of beamed, sloped ceilings on sensor placement.

A multiyear, International Fire Detection Research Project sponsored by the National Fire Protection Research Foundation (NFPRF) was initiated to provide quantitative information on the impact of beams, ceiling slope, and forced ventilation on the movement of smoke. During the first year of the project, numerical modeling was validated and additional simulations of level, beamed ceilings were completed[1] . This report describes the results of the second year of the project. During the second year, numerical simulations of smoke movement in response to sloped, beamed ceilings were studied. Based on the projected smoke movement, activation times of smoke and heat sensors were calculated. Recommendations on sensor selection and placement were made based on the activation studies.

2   Modeling assumptions

Release 3.2.1 of CFDS-FLOW3D[2] was used to perform the numerical simulations. This release is an upgrade of release 2.3.2 which was used to do the simulations for the level beamed ceilings during the first year of the project. The major improvement in the new release is in the software used to set up the geometry for the calculation. The new release introduces a multi-block grid system and grid generator which simplifies developing complex grids and eliminates wasted grid cells on interior solids.

2.1   Conservation Equations

The modeling technique used to simulate smoke flow is to divide the region of interest into a collection of small rectangular boxes or control volumes. The conditions in each control volume are initially ambient. Heat is then released in several control volumes over time. The resulting flow or exchange of mass, momentum and energy between control volumes is determined so that these three quantities are conserved. The momentum conservation or Navier Stokes equations are equivalent to Newton's second law of motion. The energy conservation equation is equivalent to the first law of thermodynamics. These

fluid flow equations are expressed mathematically as a set of simultaneous, non-linear partial differential equations. After being discretized, the resulting finite volume equations are solved iteratively using a variant of Newton's method for computing coupled non-linear algebraic equations.

2.2 Turbulence

The control volume size needs to be consistent with the scale size of the phenomena of interest. Applying this criteria to turbulent flow would result in problems with many more control volumes than could possibly be solved with today's computers. As a result, turbulence models have been developed to account for the effect of small-scale fluid motion on motion in the larger-scale control volumes. The turbulence model used for this work is the K-ϵ model[2] which was initially developed in the early seventies. This model has a number of empirical parameters which effect the ultimate viscosity and heat transfer in the plume. The default model in CFDS-FLOW3D uses the original empirical parameters proposed by Launder and Spalding[3] and these were used in the smoke movement studies conducted during the first year of this project. Other sets of parameters, which included the production of turbulence by buoyancy and a set of parameters proposed by Nam and Bill[4] based on plume correlation studies, were tried but produced only small differences with the results using the default parameters. A recent comparison given in reference [5] of a numerical simulation of a 30.4 m plume with experiment suggests that the parameter set of Nam and Bill may be superior to the default parameters, and were used in the present calculations.

2.3 Heat Transfer

Solid surfaces for all cases where the beams were parallel to the slope were assumed to be adiabatic. Clearly in actual building fires, heat is transferred between the gas and the walls. This adiabatic assumption will result in warmer gas temperature predictions since no convective heat transfer occurs between the gas and the walls. Several runs were made to examine the significance of the adiabatic assumption.

With beams perpendicular to the slope of the ceiling there is a greater chance for error from an adiabatic assumption since the gas remains in contact with the beamed ceiling for a longer period of time. To test whether the adiabatic assumption was reasonable, both conducting and non-conducting ceiling cases were modeled using the thermal properties for wall board. For both smoke and thermal devices predicted gas temperatures and sensor activation times were not significantly affected by the adiabatic assumption. Figures 11(a) and 11(b) show smoke detector response for cases 39 and 39a respectively. Cases 39 and 39a are identical except that case 39 includes heat transfer between the smoke and the walls, ceiling and beams. Note the small variation in predicted smoke detector response

3

in the center of the fire channel. Similarly for heat sensors, Figures 11(c) and 11(d) (the latter including heat conduction) show only a minor variation in the predicted heat sensor response.

For wall materials that are nearly insulating, the wall temperatures will quickly rise to the gas temperature, which reduces the heat transfer. The time period over which a parcel of gas is in contact with the wall surface is on the order of seconds. From these two observations and the fact that the perpendicular beam case was not significant, we conclude that the adiabatic assumption is reasonable.

Radiation effects were not included explicitly in the calculation except that only a fraction of the heat release rate was assumed to contribute to convective heating of the smoke and air. The rest of the heat was considered to be radiated away. The radiative fraction was taken to be 0.35[6, page II-18] for all simulations.

2.4   Grid and Boundary Specifications

Ceilings with slopes of 10, 25, and 50 degrees and ceiling heights measured from the fire base of 3.3 m (11 ft) and 4.6 m (15 ft) were simulated. A number of different grids were required to represent these geometries. Each of the grids used in the study was prepared with the grid generator, SOPHIA, which is part of the CFDS-FLOW3D software package. The multi-block feature of the package enabled the portion of the grid containing the fire to be identical for all simulations. The total number of grid cells used to represent the various geometries varied from 13000 to 25000. Cases simulated with fewer grid cells were used to minimize computer processing time and resulted in a savings of about a factor of 2 compared with the more finely gridded cases. However, such savings could only be achieved with cases involving simple geometries without encountering errors related to insufficient gridding. Grid spacing within a single block was varied using geometric progressions. Grid cells within the plume region were chosen to minimize abrupt size changes which could produce numerical problems. Each grid was comprised of three segments based on height. The lowest segment consisted of a minimum of 6 blocks and was a rectangular, non-uniform grid. The middle segment had the same number of blocks as the lowest segment and produced the transition between the lower rectangular grid and the desired slope. The highest segment was comprised of at least the same number of blocks as the other two segments and was sloped at a constant angle. It is in this segment that the beams were placed. An example grid for 25 degree slope cases is shown in Figure 1.

Several choices had to be made regarding how to handle boundary conditions for the sloped ceiling simulations. It was decided to make the boundary at the low end of the sloped ceiling a wall and not include any venting at the wall. The fire was located 2.1 m (6.9 ft) from the low wall for the 10 and 25 degree cases and 1.8 m (5.9 ft) from the low wall for the 50 degree slope. The fire was centered on a symmetry plane for all three series of sloped ceiling cases. The side opposite the symmetry plane was also chosen to be a wall

and was located at a distance of 7.3 m (24 ft) from the symmetry plane. The high side of the slope was a combination of wall and open boundary conditions. It was necessary to provide some venting of smoke; otherwise the enclosure would eventually fill with smoke. Since open boundary conditions always represent approximations to the fluid flow, it was desired to have the open boundaries far from the fire. The open boundaries or vents were chosen to be on the same level as the blocks which contained the beams. Depending on the grid, the position of the vents ranged from 8.9 m (29 ft) to 14 m (46 ft) from the fire center. Two different venting areas were used with only the perpendicular faces open in one case and both the perpendicular and bottom faces open in others. The increasing grid cells associated with the middle level blocks introduce potential for numerical error and so were terminated with wall boundary conditions. The wall was extended to the floor such that the only venting allowed in the computation was near the ceiling.

Ceiling beams were represented by thin surfaces. A *thin surface* is terminology used by CFDS-FLOW3D to describe a mechanism for preventing fluid from moving directly from one grid cell to another. Conceptually, it can be thought of as a wall between grid cells. It effectively sets the perpendicular component of the velocity to zero at the surface. Thin surfaces were used to model beams because they minimized the number of grid volumes which in turn resulted in more efficient problem solutions. The error in spatial resolution (less than 0.305 m) introduced by the thin surfaces was not thought to be significant. A minimum of 4 grid cells were used to represent the 0.10 m (4.0 in), 0.15 m (6.0 in), 0.20 m (8.0 in) and 0.30 m (12. in) beams with 6 grid cells usually representing the 0.46 m (18. in) and 0.61 m (24. in) beams. The grid cells in the beam region were usually increased in size using geometric progressions such that the smallest grid cells were located near the ceiling.

The region below the high end of the sloped ceiling and far from the fire did not significantly affect flow either below the ceiling or near the fire. Therefore this region was not included in the calculations in order to save computer time.

2.5 Fire

The fire used in all the simulations was a medium growth 't^2' fire which was designed to reach 1.055 MW (1000. Btu/s) in 275 seconds [7, B-2.2.3.2.2, pg 72-159]. The medium growth curve represents the broadest range of actual fires which might be encountered in practice. In addition, the previous study[1] showed that the results were not sensitive to the fire growth rate.

The fire was modeled by releasing energy over several grid cells. The number of grid cells occupied by the fire was varied during the simulation such that the maximum energy release per volume would be about 2.6 MW/m^3 which approximates the heat release rate of a 0.46 m (1.5 ft) high stack of wood pallets[8]. The fire was situated at the symmetry plane for the enclosure and was located away from the boundaries (as specified in Section

2.4). To account for radiative losses from the fire, 35 per cent of the heat release rate was assumed lost to the walls and ceiling through radiation.

3 Case Study

3.1 Scope

This study was designed to demonstrate how beam depth, beam spacing, and ceiling height impacted heat and smoke movement for sloped ceilings. Ceiling slopes of 10, 25, and 50 degrees were studied for beams running parallel to the slopes at depths of 0.10, 0.20, 0.30 and 0.61 m (4.0, 8.0, 12., and 24. in), beam spacings of 1.2 m and 2.4 m (4 ft and 8 ft), and ceiling heights of 3.4 m and 4.6 m(11 ft and 15 ft). Beams running perpendicular to a 25 degree slope were studied for beam depths of 0.15, 0.30, and 0.46 m (6.0, 12., and 18. in).

Special cases with gaps between the beam and the ceiling were studied for a ceiling slope of 50 degrees and a beam spacing of 1.22 m (4 ft), for beams parallel to the ceiling and a ceiling slope of 25 degrees and a beam spacing of 2.4 m (8 ft) and for beams perpendicular to the ceiling.

Ceiling slopes of 10, 25 and 50 degrees with no beams, *ie* smooth ceiling cases, were included and several of the beamed ceiling cases were done with two different venting configurations.

In all, 36 different cases are summarized in Tables 1 through 5.

Table 1: Description of Numerical Experiments Performed in Case Study - 25 Degree Cases

Cases	beam depth	beam spacing	ceiling height
1	0.10 m (4 in)	2.4 m (8 ft)	3.4 m (11 ft)
2	0.20 m (8 in)	2.4 m (8 ft)	3.4 m (11 ft)
3	0.30 m (12 in)	2.4 m (8 ft)	3.4 m (11 ft)
4	0.61 m (24 in)	2.4 m (8 ft)	3.4 m (11 ft)
6	0.20 m (8 in)	1.2 m (4 ft)	3.4 m (11 ft)
8	0.61 m (24 in)	1.2 m (4 ft)	3.4 m (11 ft)
9	0.20 m (8 in)	2.4 m (8 ft)	4.6 m (15 ft)
10	0.30 m (12 in)	2.4 m (8 ft)	4.6 m (15 ft)
11	0.61 m (24 in)	2.4 m (8 ft)	4.6 m (15 ft)
12	0.20 m (8 in)	1.2 m (4 ft)	4.6 m (15 ft)
13	0.30 m (12 in)	1.2 m (4 ft)	4.6 m (15 ft)
40	no beams		3.4 m (11 ft)

Table 2: Description of Numerical Experiments Performed in Case Study - 10 Degree Cases

Cases	beam depth	beam spacing	ceiling height
14a	0.30 m (12 in)	2.4 m (8 ft)	3.4 m (11 ft)
15	0.61 m (24 in)	2.4 m (8 ft)	3.4 m (11 ft)
16	0.20 m (8 in)	2.4 m (8 ft)	3.4 m (11 ft)
17	0.20 m (8 in)	1.2 m (4 ft)	3.4 m (11 ft)
18a	0.30 m (12 in)	1.2 m (4 ft)	3.4 m (11 ft)
19	0.61 m (24 in)	1.2 m (4 ft)	3.4 m (11 ft)

Table 3: Description of Numerical Experiments Performed in Case Study - 50 Degree Cases

Cases	beam depth	beam spacing	ceiling height
20	0.30 m (12 in)	2.4 m (8 ft)	4.6 m (15 ft)
21	0.20 m (8 in)	2.4 m (8 ft)	4.6 m (15 ft)
22	0.10 m (4 in)	2.4 m (8 ft)	4.6 m (15 ft)
23	0.30 m (12 in)	2.4 m (8 ft)	4.6 m (15 ft)
24	(no beams)		4.6 m (15 ft)
25	0.20 m (8 in)	1.2 m (4 ft)	4.6 m (15 ft)
27	0.30 m (12 in)	1.2 m (4 ft)	4.6 m (15 ft)
28	0.30 m (12 in)(3 in gap)	1.2 m (4 ft)	4.6 m (15 ft)
29	0.10 m (4 in)	1.2 m (4 ft)	4.6 m (15 ft)
30	0.30 m (12 in)	2.4 m (8 ft)	4.6 m (15 ft)

Table 4: Description of Numerical Experiments Performed in Case Study - Perpendicular Beams, 10 degree slope

Cases	beam depth	beam spacing	ceiling height
41	0.36 m (14 in)	2.4 m (8 ft)	3.4 m (11 ft)
42	0.30 m (12 in)	2.4 m (8 ft)	3.4 m (11 ft)

Table 5: Description of Numerical Experiments Performed in Case Study - Perpendicular Beams, 25 degree slope

Cases	beam depth	beam spacing	ceiling height
37	0.30 m (12 in)	2.4 m (8 ft)	3.4 m (11 ft)
38	(6 in)	2.4 m (8 ft)	3.4 m (11 ft)
39	(18 in)	2.4 m (8 ft)	3.4 m (11 ft)
39a (conducting walls)	(18 in)	2.4 m (8 ft)	3.4 m (11 ft)
43	0.30 m (12 in)	2.4 m (8 ft)	3.4 m (11 ft)
44	0.45 m (18 in)(5 inch gap)	2.4 m (8 ft)	3.4 m (11 ft)

3.2 Analysis

Detector activation was calculated in the following manner. For smoke detectors, it was assumed that particle density would correlate with temperature and that smoke detectors would activate when the temperature reached a value of 13° C above ambient [9]. For heat sensors, the activation temperature was chosen to be 57° C (135° F) and the thermal inertia of the sensing element to be represented using the differential equations developed in[10].

$$\frac{dT_L}{dt} = \frac{\sqrt{U(t)}}{\text{RTI}}(T_g(t) - T_L(t)),$$
$$T_L(0) = T_g(0)$$

where T_L, T_g are the link and gas temperatures in ° C, U is the flow speed of the gas (magnitude of flow velocity) and RTI is a measure of the sensor's sensitivity to temperature change (thermal inertia). RTI values used in these studies included 50, 100, and 300 $(\text{m s})^{.5}$. This model assumes that forced convection is the dominant mode of heat transfer and ignores heat loss due to radiation and conduction.

The velocity and temperature predictions were used to calculate activation times of smoke detectors and heat sensors at every grid volume in the computational space. The effects of ceiling slope, ceiling height, beam depth, and beam spacing were analyzed by studying how the sensor activation volume changed as these parameters were modified. The sensor activation volume is that volume which encloses all grid cells that show the activation of a particular sensor for a given fire size. Target fire sizes of 100 kW and 1.0 MW were used to study the activation volumes produced by the growing fire. The ambient temperature used for all calculations was 20° C, hence smoke detectors were assumed to activate when the temperature in a particular grid volume reached 33° C.

3.3 Predicting Smoke Detector Activation

In the first and second year's work, the activation of smoke detectors (of any type) is predicted to occur at a 13° C temperature rise. This criteria is based on the work of Evans and Stroup in [11] which used Heskestad's correlation in the original Fire Detector Institute (FDI) work [12].

Heskestad proposed another smoke detector response model [13] which depends on empirical constants derived for each model of sensor. This model, when the empirical constants are truncated to a single parameter which is then held constant for all cases, yields the 13° C criterion that has been used here. Other models exist for ionization chambers (*e.g.* [14]) but for optical (scattering) sensors, only complex theory depending on particle size and refractive index is available, and is not practical in the present work.

9

One such model with potential was developed by Yamauchi [15] which relates optical sensor response to mass density and ionization to number density; both parameters which can be calculated for the cases studied. This model was verified against limited experimental data in the original report.

A similar model is currently being incorporated into the CFAST model[16] at NIST. The project team proposes to extend this work by incorporating the final version of the CFAST algorithm into the data analysis for the year 3 cases for comparison to the results analyzed with the 13° C criterion. This can be done for the optical sensors in year 3 and for ionization type in year 4. This additional year is due to of the additional complexity of dealing with particle coagulation.

4 Observations

4.1 Beams Parallel to the Ceiling Slope

Many of the observations stemming from these calculations occur due to the presence of a parallel component of the buoyant force lying along the sloped ceiling. This force component produces an asymmetrical flow situation where flow down the sloped ceiling is slowed while flow up the sloped ceiling continues to be accelerated. This effect has been documented experimentally for sloped, smooth ceilings in [17].

Observation 1 Beams trap flow more effectively as the ceiling slope is increased. Beams which may not be deep enough to trap flow on ceilings with only small slopes may be extremely effective in trapping flow as the ceiling slope is increased. Figure 2 compares the trapping capability for 0.30 m (12 in) beams for 10, 25 and 50 degree sloped ceilings with beams 2.4 m (8 ft) on center at a fire size of 100 kW. For the 25 and 50 degree ceiling slope, the smoke detectors will activate in only the first channel while for the 10 degree ceiling slope, smoke detectors will activate in the first and second channels since at this slope, the beams are not as effective at constraining the hot gas flow.

Observation 2 The greater the ceiling slope, the less the flow penetrates down the slope from the fire center. Figure 2 compares the penetration distance from plume center for a 10 degree sloped ceiling and a 25 degree sloped ceiling for a ceiling height of 3.4 m (11. ft), beam depth of 0.30 m (12.0 in), beam separation of 2.4 m (8.0 ft), and fire size of 100 kW. For the 10 degree ceiling, smoke detectors would activate nearly to the back wall, while for the 25 degree ceiling, sensor activation stops approximately 1.0 m (3.28 ft) from the back wall. Very little down slope penetration is observed for the 50 degree slope case.

Observation 3 For all cases analyzed, only smoke detectors will activate at the 100 kW fire size. Fusible link activation has not occurred at either 3.4 m (11.0 ft) or 4.57 m (15.0 ft) ceiling heights at this fire size.

Observation 4 Smoke detector activation for 100 kW fires will occur at substantial distances upslope of the plume center for all ceiling slope cases. Figure 2 shows the smoke detector activations for the 100 kW fire size for .305 m (12.0 in) beams, beam separation 2.4 m (8.0 ft) and ceiling slopes of 10, 25 and 50 degrees. In each instance, smoke detector activation occurred in excess of 4.0 m (13. ft) from plume center.

Observation 5 Activation conditions under beams may be equivalent to activation conditions in adjacent beam channels. Figures 3 and 4 show the response volumes for a number of different beam configurations and sensors. In all instances, when a sensor activates in an adjacent beam channel, it will have activated if placed 0.076 m (3.0 in) under the beam. The activation volume may be smaller under the beam than in the adjacent channel.

Observation 6 The speed of the gas decreases as the plume nears the ceiling but then accelerates along the ceiling slope as shown in Figure 5 for a 50 degree sloped ceiling.

Observation 7 For 10 degree ceiling slope, heat sensor activation at the 1 MW fire size occurred in the fire channel and the two adjacent channels at all beam depths for RTI 50 $(m\,s)^{1/2}$ and RTI 100 $(m\,s)^{1/2}$ heat sensors. Activation only occurred in the fire channel for the RTI 300 $(m\,s)^{1/2}$ sensor. Smoke detector activation occurred in the fire channel and the two adjacent beam channels for the 100 kW fire size with the exception of 0.61 (24 in) beam depths at 2.4 (8.0 ft) on center beam spacing.

Observation 8 For 25 degree ceiling slope, smoke detector activation occurs in only a single channel for beam depths greater than 0.2 m (8 in) for beam separations of both 1.2 m (4 ft) and 2.4 m (8 ft) on center at 100 kW fire size.

Heat sensor activation with RTI 50 $(m\,s)^{1/2}$ occurred in two beam channels for a beam depth of 0.2 m (8 in) for beams spaced 1.2 m (4 ft) and 2.4 m (8 ft) on center but in only one channel for deeper beams at 1 MW fire size. Heat sensor activation occurred in only one beam channel for RTI 100 $(m\,s)^{1/2}$ and RTI 300 $(m\,s)^{1/2}$ sensors with the exception that RTI 100 $(m\,s)^{1/2}$ sensors activated in two channels for 0.2 m (8 in) beams at 1 MW fire size.

Observation 9 For 50 degree ceiling slope, smoke detector activation occurred in only one beam channel except for 0.1 m (4 in) beams, 1.2 m (4 ft) on center where activation occurred in two beam channels at 100 kW fire size. Heat sensor activation occurred in one beam channel for all RTI's except for 0.1 m (4 in) beams, 1.2 m (4 ft) on center and RTI 50 $(m\,s)^{1/2}$ for 1 MW fire size.

4.2 Beams Perpendicular to the Ceiling Slope

Perpendicular beams cause the gas flow to be, in part, redirected along the beams. The component of the buoyant force parallel to the ceiling will still be a factor in accelerating the gas along the ceiling slope. Since there is significant flow directed along the beam, the presence of a wall will stop the gas flow along the beam and make it move up over the beam

at the wall location.

Observation 10 Perpendicular beams impede the flow up the ceiling. The 0.15 m (6 in) beams permit more flow than the 0.30 m (12 in) and 0.45 m (18 in) beams which tend to channel more flow along the beams as shown in Figure 6.

Observation 11 For the 0.30 m (12. in) and 0.46 m (18 in) beams, the interaction of the flow with the side wall produces the most significant upslope flow (see Figure 7).

Observation 12 When the upslope flow starts to fill a higher beam channel, conditions for detection 0.076 m (3.0 in) beneath the beam are equivalent to the conditions in the higher channel. (See Figures 8(a) and 8(c).

Observation 13 Comparison of conducting and non-conducting ceilings (See Figure 11.) demonstrated that the adiabatic assumption was reasonable.

Observation 14 Increasing the ceiling slope decreases the effectiveness of the perpendicular beams in impeding the flow of smoke up the ceiling. Figure 9 shows the temperature profile in a vertical plume 0.1 m (4 in) offset from the plume center for the 100 kW and 1 MW fire sizes at 10 and 25 degree ceiling slopes. The lower slope allows the hot gas to flow over the down slope beam. Upstream penetration is more pronounced and is particularly evident in Figure 10 which shows RTI 50 $(m\,s)^{1/2}$ fusible links activating one beam channel further along the ceiling for the 25 degree slope than for the 10 degree slope.

Observation 15 For 10 degree ceiling slope, smoke detectors will activate in two or more channels for 100 kW fire size and 0.30 m (12 in) beams. Thermal sensors with RTI of 50 and 100 will activate in two beam channels but sensors with RTI 300 $(m\,s)^{1/2}$ will activate in only one beam channel at the 1.0 MW fire size.

Observation 16 For 25 degree ceiling slope, smoke detectors will activate in two or more beam channels for beam depths of 0.15 m (6 in), 0.30 m (12 in) and 0.45 m (18 in) at 100 kW fire size. Heat sensors with RTI 50 $(m\,s)^{1/2}$ will activate in two channels for all beam depths, RTI 100 $(m\,s)^{1/2}$ will activate in two beam channels for 0.15 m (6 in) and 0.3 m (12 in) beams but in only one beam channel for 0.45 m (18 in) beams and RTI 300 $(m\,s)^{1/2}$ sensors will activate in only one beam channel.

4.3 Parallel Beams With Gaps

The presence of a gap between the top of the beam and the ceiling should provide some access for gas flow into adjacent beam channels. The simulation used for this study was a 50 degree sloped ceiling with 0.30 m (12. in) beams 1.22 m (4.0 ft) on center with the beams running parallel to the slope. The gap was located next to the ceiling and was 0.076 m (3.0 in) deep. Two grid cells represented the gap while the beam was represented by an additional four grid cells using a geometrical progression.

Observation 17 The gap allows the gas flow to reach additional adjacent channels. Figure 12 gives a comparison between the flow with and without a gap for 100 kW and 1

MW fires. For each fire size, the presence of the gap allows smoke detectors to activate in an additional adjacent channel.

Observation 18 The upslope activation of smoke detectors and heat sensors is decreased when a gap is present. See Figures 12 and 13.

Observation 19 The presence of a gap does not permit activation of heat sensors in additional beam channels for the 1 MW fire size. See Figure 13.

4.4 Perpendicular Beams With Gaps

The presence of a gap between the top of a beam and the ceiling should permit hot gas flow to move more freely in the upslope direction. The simulation used to study this case was a 25 degree sloped ceiling with a 0.13 m (5 in) gap in an 0.46 m (18 in) beam.

Observation 20 The gap permitted more rapid flow up the ceiling slope. Comparing contour plots in Figure 14 show activation at larger distances from the plume center for both smoke detectors and heat sensors.

Observation 21 The gap permitted downslope flow with activation of smoke detectors and heat sensors in beam channels below the plume center as shown in Figures 14(b), 14(d) and 15(b).

Observation 22 The presence of the gap reduces the thickness of the activation region underneath the beams as shown in Figures 14(b) and 14(d).

5 Conclusions

Figure 16 presents a schematic diagram of a sloped ceiling enclosure. It illustrates terms used in making some of the following conclusions.

As in the first year report[1], optimum sensor locations were determined for two design fire sizes of 100 kW and 1 MW, for smoke detectors and for thermal sensors with response time indices (RTI) of 50, 100, and 300. Further, as shown in that study, when based on activation before reaching a specific design fire size, the results are insensitive to fire growth rate; the time to activation varies with the time to reach the design fire size for each growth rate.

The series of figures presented show response volumes for specified combinations of sensor, beam depth and spacing, beam orientation, ceiling slope, design fire size, and locations of 0.076 m (3 in) below the ceiling (within the beam pocket) or below the bottom of the beams. Sensors located anywhere within this response volume will have responded prior to the fire reaching the design fire size.

The sensitivity of the smoke detector response volume size to the smoke detector activation criterion (13 ° C) can be estimated by examining Figures 2, 3, 4, 6, 11 and 12. In these figures, the red region corresponds to locations where smoke detectors activate

according to the 13 ° C criterion. The yellow and green regions correspond to where smoke detectors activate using the 10 ° C and 8 ° C criterion respectively. Note that the size of the additional region encompassed by the cooler smoke temperatures is small. Since the observations in the previous section and the conclusions in this section are based on the size and location of the smoke detector response volume the conclusions would not change as a result of using activation criterion as low as 8° C.

It was generally observed that increasing the ceiling slope caused the flow velocity up the slope to increase. When the beams run parallel to (up) the slope, they channel the flow, causing it to accelerate more. The effect is similar to that observed in the first year with horizontal, beamed ceilings for the flow in the direction parallel to the beams, but more pronounced due to the acceleration of the flow up the slope. This increased flow channeling is insensitive to the depth of the beams over the range of beam depths studied. Increasing the slope also decreases the downslope penetration of the flow, so that for slopes greater than 10° the row of sensors at the low end of the sloped ceiling (located half the spacing from the wall) are unlikely to activate unless the fire is very near the lower wall, and then the accelerated flow would cause the next row up the slope to activate quickly. Thus, in these cases it is felt that this lowest row of sensors may be omitted.

When the beams run perpendicular to (across) the slope they impede the flow and cause it to slow in the up slope direction and spread further across the ceiling within the channel. Again, the effect is similar to the horizontal, beamed ceiling with the flow component perpendicular to the beam direction. Here, the beam depth influences the effect since deeper beams produce more channeling, but the effect of the ceiling slope is reduced as the flow has less chance to accelerate before being turned by the beam.

In the current National Fire Alarm Code (1993 edition), sensor spacing on sloped ceilings is measured on a horizontal projection of the ceiling. This increases the spacing between sensors up the slope by $1/\cos(\theta)$ as the slope increases. The present results indicate that this is appropriate since the increasing slope accelerates the flow and causes the response volume to expand. Thus the spacing recommendations below are based on measurements projected to the horizontal. These recommendations are presented in code language so that dimensions are unambiguous to code committees considering adoption. The wording is suggested and should be modified for clarity and to conform to required style if needed.

Spacing Recommendations
For smoke detectors and 100 kW design fires:

The recommendation from year 1 for horizontal, beamed ceilings was:

For ceiling heights of 3.66 m (12 ft) or lower, and beam depths of 0.305 m (1 ft) or less, smooth ceiling spacings shall be used in the direction parallel to the run of the beams and half the smooth ceiling spacing in the direction perpendicular to the run of the beams. Detectors shall be located either on the ceiling or on the bottom of the beams. For beam

depths exceeding 0.305 m (1 ft) or for ceiling heights exceeding 3.66 m (12 ft), smoke detectors shall be located on the ceiling in every beam pocket.

The corresponding recommendation for sloped, beamed ceilings with beams running parallel to (up) the slope is as a result of the year 2 work is:

The spacing for horizontal, beamed ceilings shall be used. The ceiling height shall be taken as the average height over the slope. For slopes greater than 10°, the sensors located half the spacing from the low end shall be permitted to be omitted. Spacings shall be measured along a horizontal projection of the ceiling.

The recommendation for sloped, beamed ceilings with beams running perpendicular to (across) the slope is:

For ceilings of any slope, the spacing for horizontal, beamed ceilings shall be used. The ceiling height shall be taken as the average height over the slope.

For smoke detectors and 1 MW design fires:

The recommendation from year 1 for horizontal, beamed ceilings was:

For ceiling heights of 8.53 m (28 ft) or less, smooth ceiling spacings shall be used and the sensors shall be permitted to be located on the ceiling or on the bottom of the beams.

The accelerated flow up the slope results in increased channeling of the flow. Thus, the recommendation for sloped, beamed ceilings with beams running parallel to (up) the slope is:

For ceiling slopes less than or equal to 10° , spacings for horizontal, beamed ceilings shall be used. For ceilings with slopes greater than 10°, twice the smooth ceiling spacing shall be used in the direction parallel to (up) the slope and half the spacing in the direction perpendicular to (across) the slope. For slopes greater than 10°, the sensors located half the spacing from the low end shall be permitted to be omitted. Spacings shall be measured along a horizontal projection of the ceiling.

The recommendation for sloped, beamed ceilings with beams running perpendicular to (across) the slope is:

For ceilings of any slope, smooth ceiling spacings shall be used in the direction parallel to the beams (across the slope), and half the smooth ceiling spacing in the direction perpendicular to the beams (up the slope).

For thermally activated devices and 1 MW fires:

The recommendation for sloped, beamed ceilings with beams running parallel to (up) the slope is:

For RTI less than or equal to 100 and slopes less than or equal to 10°, smooth ceiling spacings shall be used in the direction parallel to the beams (up slope), and half the smooth ceiling spacing in the direction perpendicular to the beams (across the slope). For RTI greater than 100 or slopes greater than 10°, smooth ceiling spacings shall be used in the direction parallel to the beams (up slope) with sensors placed within every beam pocket or

on the bottom of every beam in the direction perpendicular to the beams (across the slope). The recommendation for sloped, beamed ceilings with beams running perpendicular to (across) the slope is:

For RTI less than or equal to 100, slopes less than or equal to 25°, and beam depths less than or equal to 0.305 m (1 ft), smooth ceiling spacings shall be used in the direction parallel to the beams (across), and half the smooth ceiling spacing in the direction perpendicular to the beams (up slope). For RTI greater than 100, slopes greater than 10°, or beam depths greater than 0.305 m (1 ft), smooth ceiling spacings shall be used in the direction parallel to the beams (across slope) with sensors placed within every beam pocket or on the bottom of every beam in the direction perpendicular to the beams (up slope).

References

[1] Glenn P. Forney, Richard W. Bukowski, and William D. Davis. Simulating the effect of flat beamed ceilings on detector and sprinkler response, 1993. Available from the National Fire Protection Association, Batterymarch Park, Quincy, MA.

[2] CFD Department, AEA Industrial Technology, Harwell Laboratory, Oxfordshire, United Kingdom. *HARWELL-FLOW3D Release 3.2: User Manual*, October 1992.

[3] B.E. Launder and D.B. Spalding. The numerical computation of turbulent flows. *Computer Methods in Applied Mechanics and Engineering*, 3:269–289, 1974.

[4] S. Nam and R. G. Bill Jr. Numerical simulation of thermal plumes. *Fire Safety Journal*, 21:231–256, 1993.

[5] Kathy A. Notarianni and William D. Davis. The use of computer models to predict temperature and smoke movement in high bay spaces. Technical Report 5304, National Institute of Standards and Technology, 1993.

[6] W.D. Walton and P.H. Thomas. Estimating temperatures in compartment fires. In Phillip J. DiNenno et al., editors, *SFPE Handbook of Fire Protection Engineering*, chapter II-2. McGraw-Hill Book Company, New York, first edition, 1989.

[7] NFPA 72, National Fire Alarm Code, 1993 edition, 1993.

[8] NFPA 204M, Guide For Smoke and Heat Venting, 1982.

[9] G. Heskestad and M. A. Delichatsios. Environments of Fire Detectors - Phase II: Effect of Ceiling Configuration. Volume I. Analysis. NBS-GCR-78-129, National Institute of Standards and Technology, 1978.

[10] Gunnar Heskestad and Herbert F. Smith. Investigation of a new sprinkler sensitivity approval test: The plunge test. Technical Report Serial No. 22485 2937, Factory Mutual Research Corporation, Norwood, MA, 1976. RC 76-T-50.

[11] D. D. Evans and D. W. Stroup. Methods to calculate the response time of heat and smoke detectors installed below large unobstructed ceilings. *Fire Technology*, 22:54–65, 1986.

[12] G. Heskestad and M. A. Delichatsios. Environments of Fire Detectors - Phase I: Effect of Fire Size, Ceiling Height and Material, Volume II. Analysis. NBS-GCR-77-95, National Institute of Standards and Technology, 1977.

[13] Gunnar Heskestad. Generalized characterization of smoke entry and response for product-of-combustion detectors. In *Fire Detection for Life Safety. March 31 - April 1*, pages 93–127. National Research Council, 1975.

[14] Charles D. Litton. Mathematical model for Ionization type smoke detectors and the reduced source approximation. *Fire Technology*, 13:266–281, 1977.

[15] Y. Yamauchi. Prediction of response time of smoke detectors in enclosure fires. Technical Report 3707, National Bureau of Standards, 1988.

[16] Richard D. Peacock, Glenn P. Forney, Paul Reneke, Rebecca Portier, and Walter W. Jones. CFAST, the consolidated model of fire growth and smoke transport. Technical Note 1299, National Institute of Standards and Technology, 1993.

[17] Hsiang-Cheng Kung, Robert D. Spaulding, and Paraskevas Stavrianidis. Fire induced flow under a sloped ceiling. In Geoffrey Cox and Brian Langford, editors, *Fire Safety Science - Proceedings of the Third International symposium*, pages 271–280, New York, 1991. International Association of Fire Safety Science, Elsevier Applied Sciences.
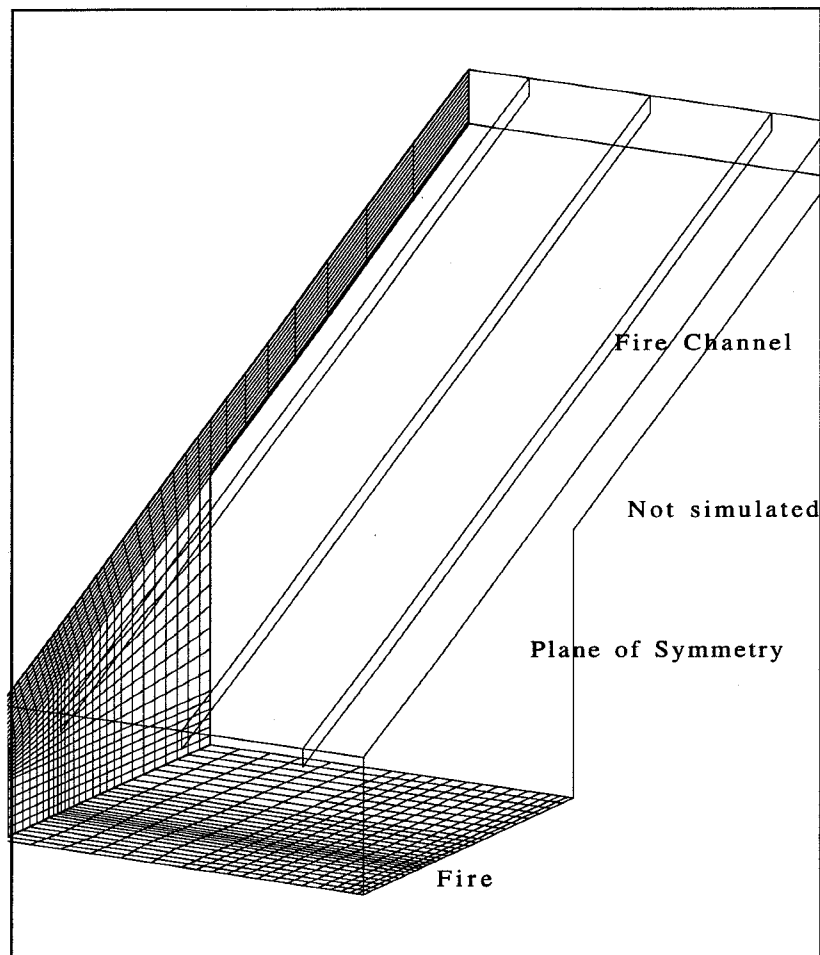
Figure 1: Grid typical of those used to simulate **25 degree** cases.
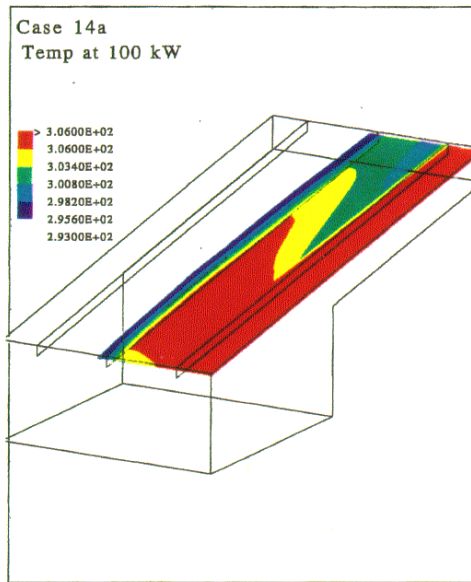
(a) 10 degree slope
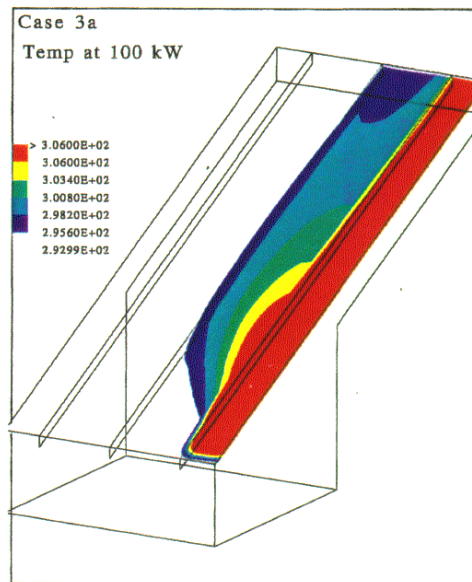
(b) 25 degree slope
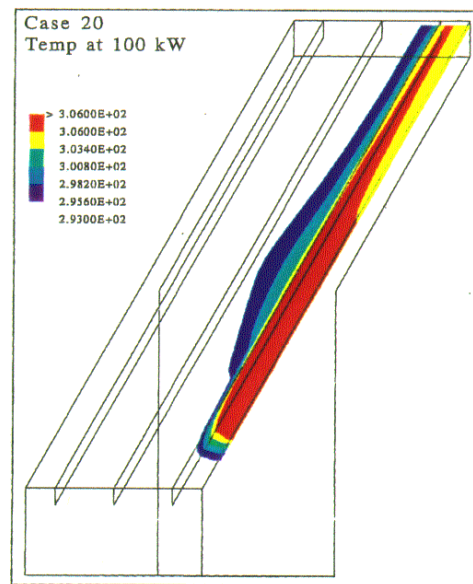
(c) 50 degree slope

Figure 2: Contour plots of **smoke** detector response for three slopes with 0.30 m (**12 in**) **deep beams** and a t^2 fire that reaches **100 kW** in 87 seconds. The plots are in a plane parallel to the ceiling 0.076 m (**3 in**) **below the ceiling**. The red contour indicates the sensor activation region.
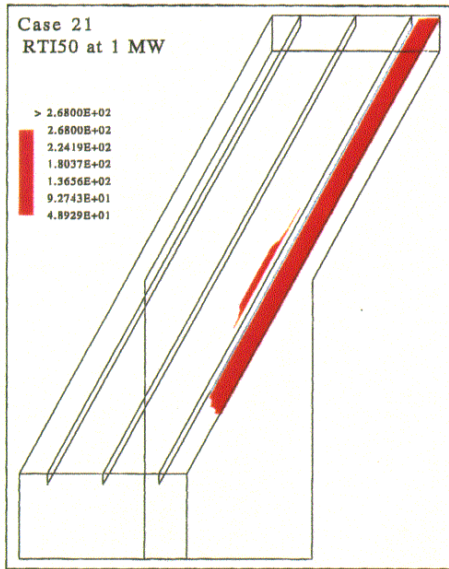
(a) RTI 50, 0.076 m (3.0 in) below ceiling
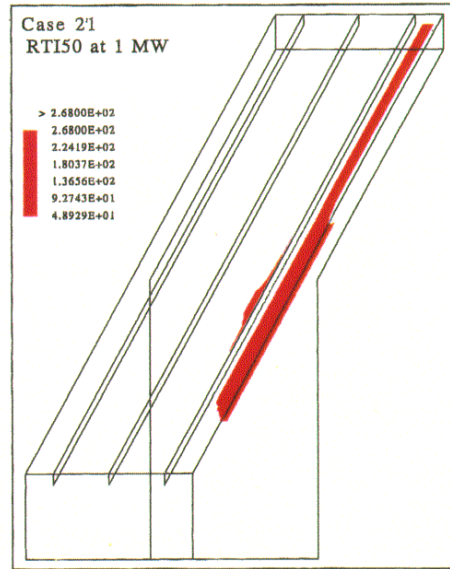

(b) RTI 50, 0.076 m (3.0 in) below beams
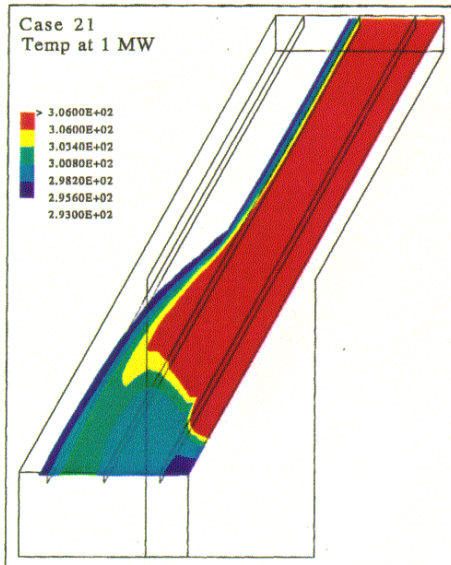
(c) Temperature, 0.076 m (3.0 in) below ceiling
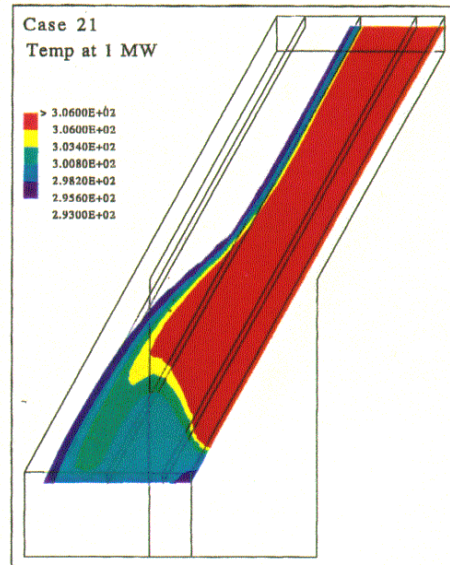
(d) Temperature, 0.076 m (3.0 in) below beams

Figure 3: Contour plots below the ceiling and below the beams of **RTI 50** $(m\ s)^{1/2}$ **heat** sensor and smoke detector response for a **50 degree** sloped beamed ceiling with 0.20 m (**8 in**) **deep beams** and a t^2 fire that reaches **1 MW** in 268 seconds. The beams are parallel to the slope of the ceiling. The red contour indicates the sensor activation region.

21
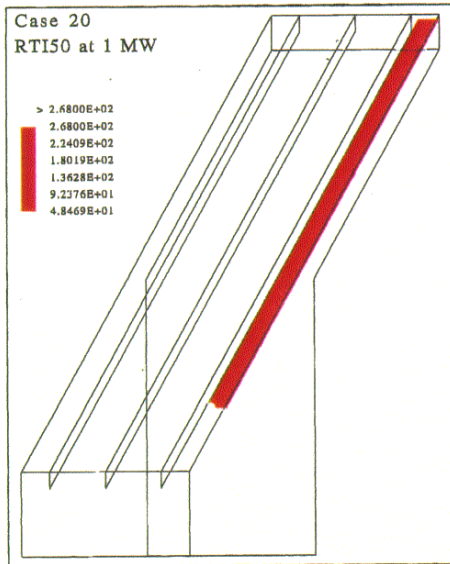
(a) RTI 50, 0.076 m (3.0 in) below ceiling

(b) RTI 50, 0.076 m (3.0 in) below beams
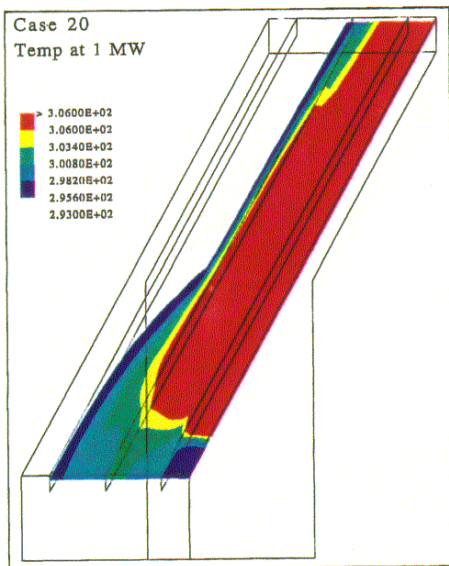
(c) Temperature, 0.076 m (3.0 in) below ceiling
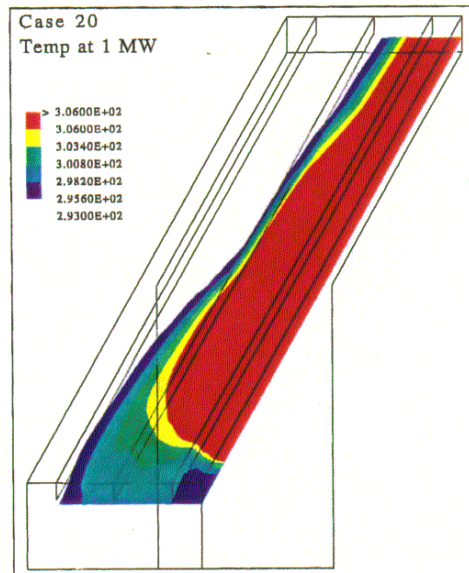
(d) Temperature, 0.076 m (3.0 in) below beams

Figure 4: Contour plots below the ceiling and below the beams of **RTI 50** $(m\ s)^{1/2}$ **heat** sensor and smoke detector response for a **50 degree** sloped beamed ceiling with 0.30 m (**12 in) deep beams** and a t^2 fire that reaches **1 MW** in 268 seconds. The beams are parallel to the slope of the ceiling. The red contour indicates the sensor activation region.

22

Case20
Speed at 1 MW

> 5.0000E+00
  5.0000E+00
  4.6250E+00
  4.2500E+00
  3.8750E+00
  3.5000E+00
< 3.5000E+00
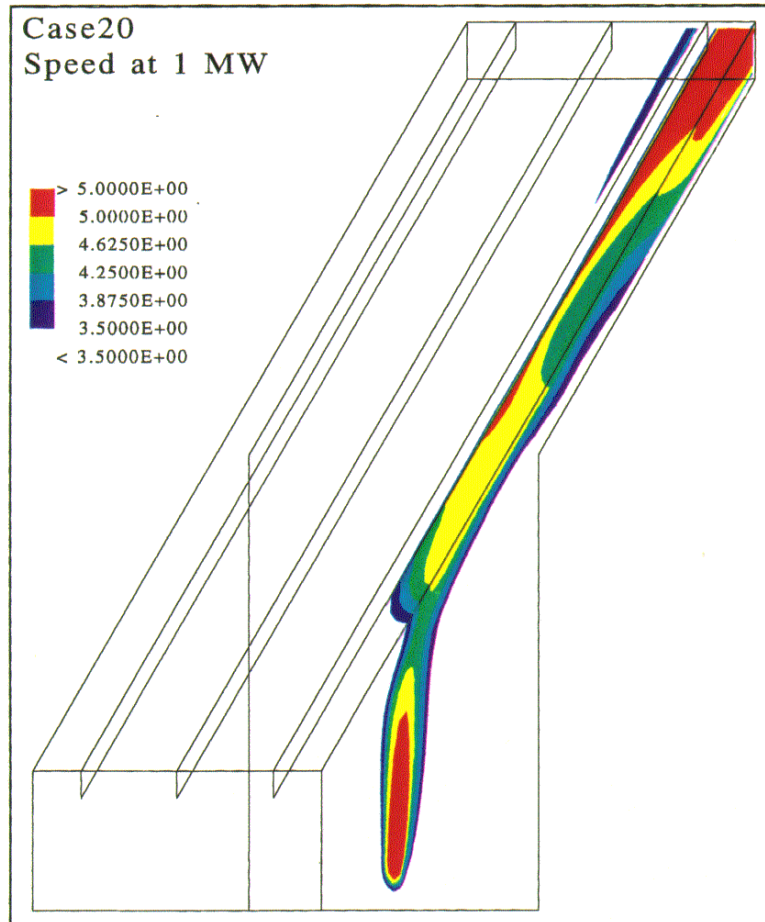
Figure 5: Contour plot of smoke **velocity** (m/s) for a **50 degree** sloped beamed ceiling with 0.30 m (**12 in**) **deep beams** and a t^2 fire that reaches **1 MW** in 268 seconds. The beams are parallel to the slope of the ceiling. The plot is in a plane parallel to the ceiling 0.076 m (**3 in**) **below the ceiling** and in a vertical plane containing the fire.
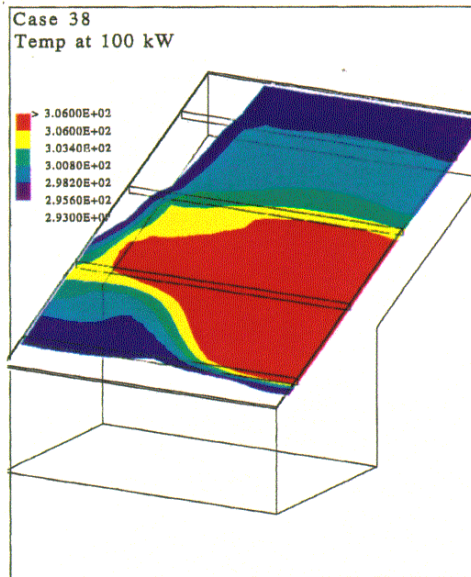
(a) 0.15 m (6 in) beam depth
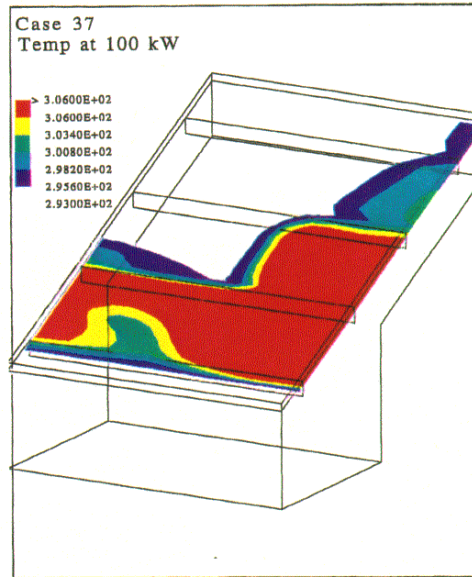
(b) 0.30 m (12 in) beam depth
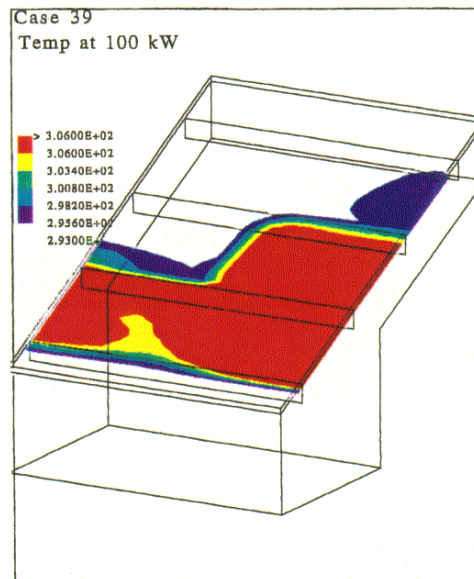
(c) 0.46 m (18 in) beam depth

Figure 6: Contour plots of **smoke** detector response for three beam depths for a **25 degree** sloped beamed ceiling and a t^2 fire that reaches **100 kW** in 87 seconds. The beams are perpendicular to the slope of the roof. The plot is in a plane parallel to the ceiling 0.076 m **(3 in) below the ceiling**. The red contour indicates the sensor activation region.

Case 37
RTI50 at 1 MW

> 2.6800E+02
2.6800E+02
2.1440E+02
1.6080E+02
1.0720E+02
5.3600E+01
0.0000E+00

Case 39
RTI50 at 1 MW

> 2.6700E+02
2.6700E+02
2.2405E+02
1.8111E+02
1.3816E+02
9.5211E+01
5.2264E+01
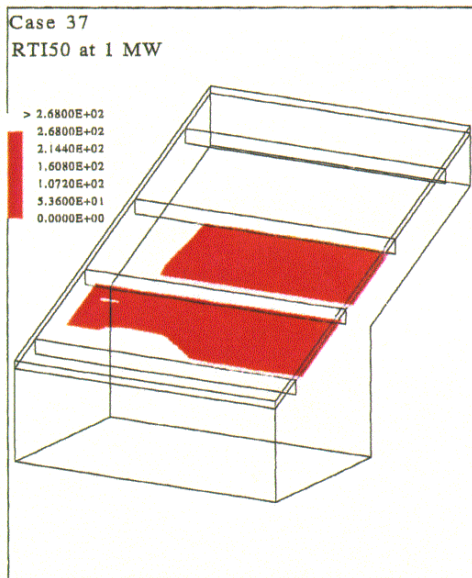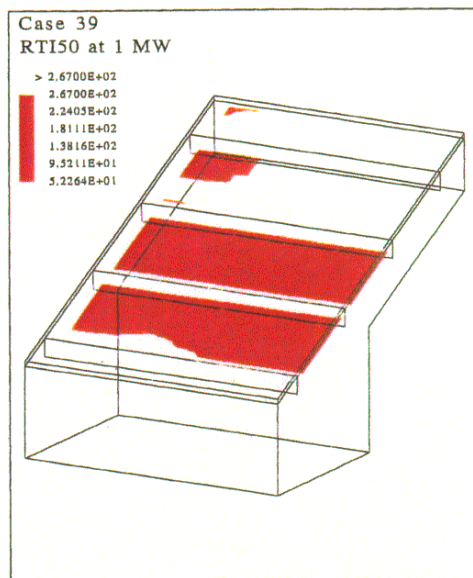
(a) 0.30 m (12 in) beam depth   (b) 0.46 m (18 in) beam depth

Figure 7: Contour plot of **RTI 50** $(\text{m s})^{1/2}$ **heat** sensor response for two beam depths for a **25 degree** sloped beamed ceiling and a t^2 fire that reaches **1 MW** in 268 seconds. The beams are perpendicular to the slope of the roof. The plots are in a plane parallel to the ceiling 0.076 m **(3 in) below the ceiling**. The red contour indicates the sensor activation region.
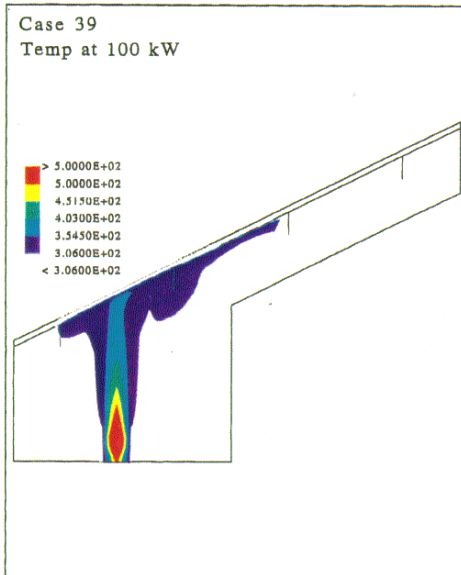
(a) Temperature, 100 kW
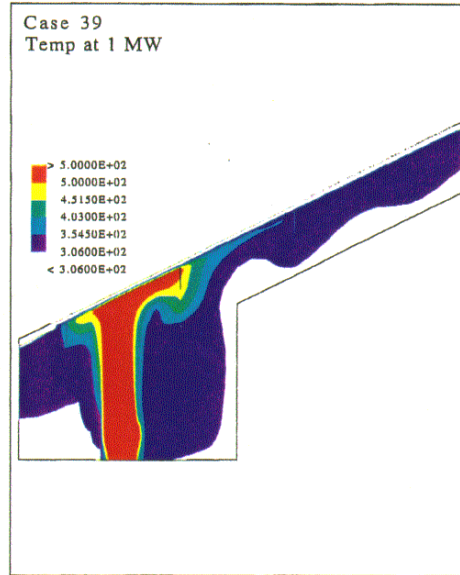
(b) Temperature, 1 MW
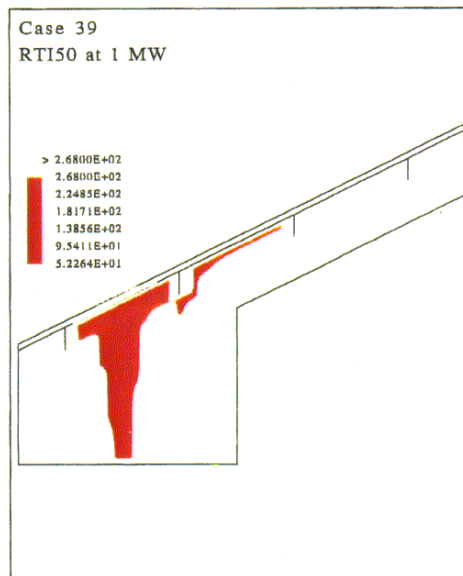
(c) RTI 50, 1 MW

Figure 8: Contour plots of **smoke** detector and **RTI 50** $(m\,s)^{1/2}$ **heat** sensor response for two fire sizes for a **25 degree** sloped beamed ceiling with 0.46 m **(18 in) deep beams**. The beams are perpendicular to the slope of the ceiling. The plots are in a vertical plane containing the fire. The Contours in (a) and (b) indicate the smoke detector activation region. The red contour in (c) indicates the heat sensor activation region.

26
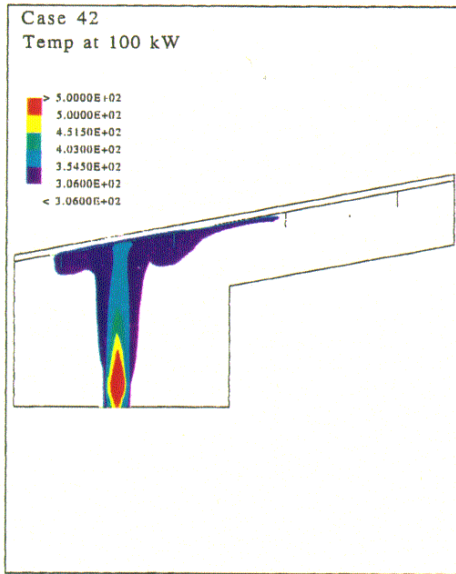
(a) 10 degree slope, 100 kW
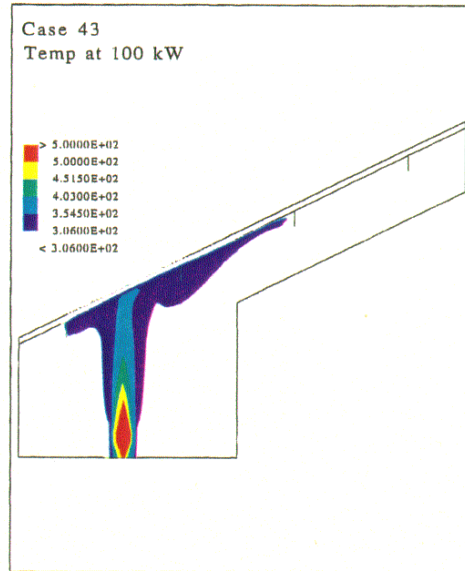
(b) 25 degree slope, 100 kW
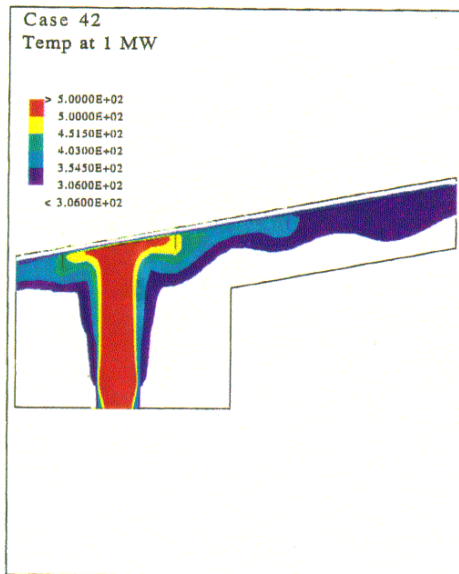
(c) 10 degree slope, 1 MW
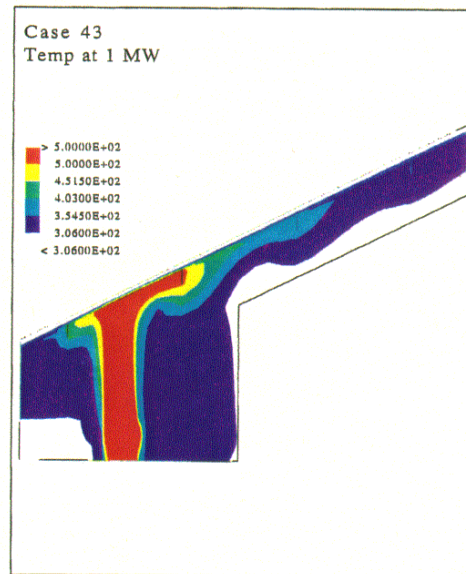
(d) 25 degree slope, 1 MW

Figure 9: Contour plots of smoke temperature for two ceiling slopes and two fire sizes and 0.30 m **(12 in) deep beams**. The beams are perpendicular to the slope of the ceiling. The plots are in a vertical plane containing the fire. The Contours indicate the smoke detector activation region.

27

Case 42
RTI50 at 1 MW

> 2.6800E+02
2.6800E+02
2.1440E+02
1.6080E+02
1.0720E+02
5.3600E+01
0.0000E+00

Case 43
RTI50 at 1 MW

> 2.6800E+02
2.6800E+02
2.2480E+02
1.8161E+02
1.3841E+02
9.5216E+01
5.2020E+01
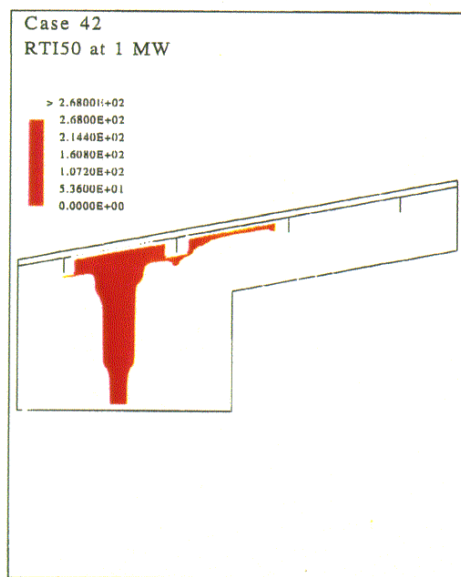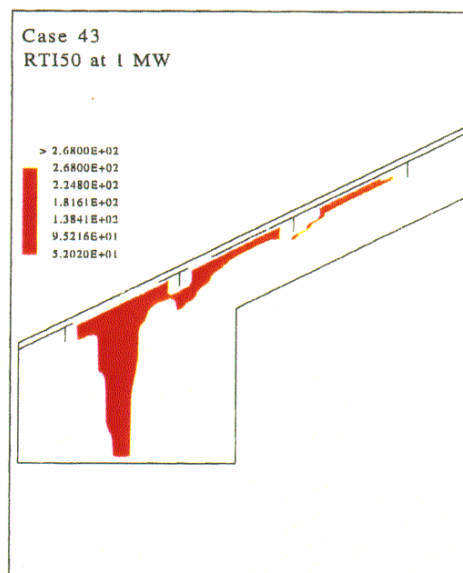
(a) 10 degree slope   (b) 25 degree slope

Figure 10: Contour plot of **RTI 50** $(\mathrm{m\ s})^{1/2}$ **heat** sensor response for two ceiling slopes with 0.30 m (**12 in**) **deep beams** and a t^2 fire that reaches **1 MW** in 268 seconds. The beams are perpendicular to the slope of the ceiling. The plots are in a vertical plane containing the fire. The red contour indicates the sensor activation region.
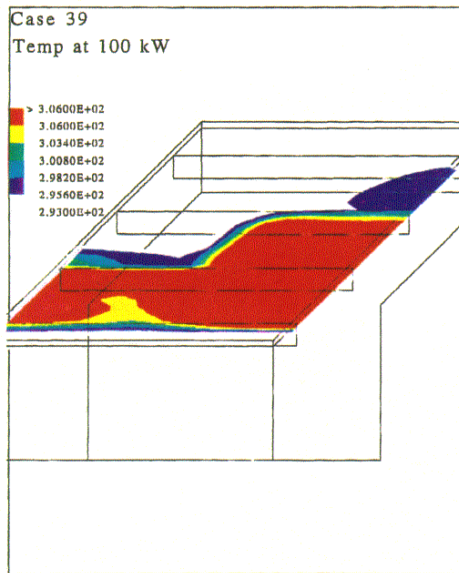
(a) 100 kW, non-adiabatic
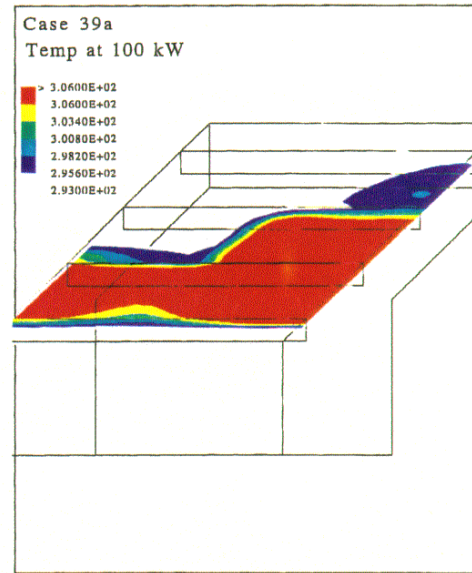
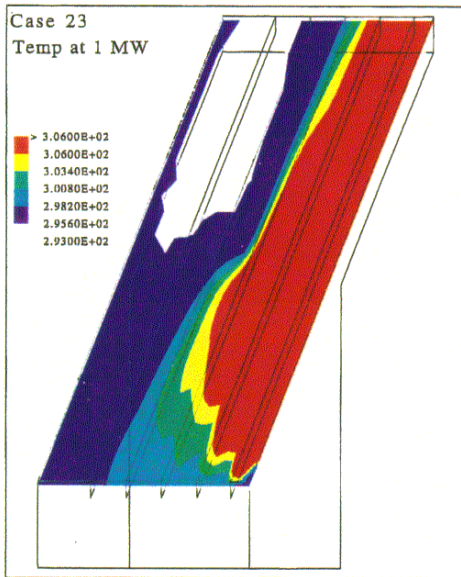(b) 100 kW, adiabatic
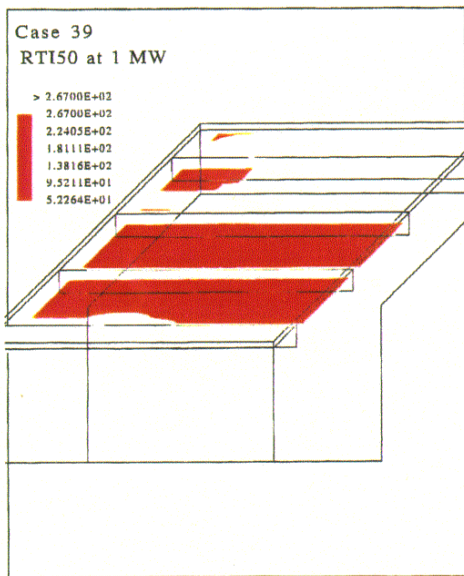
(c) 1 MW, non-adiabatic
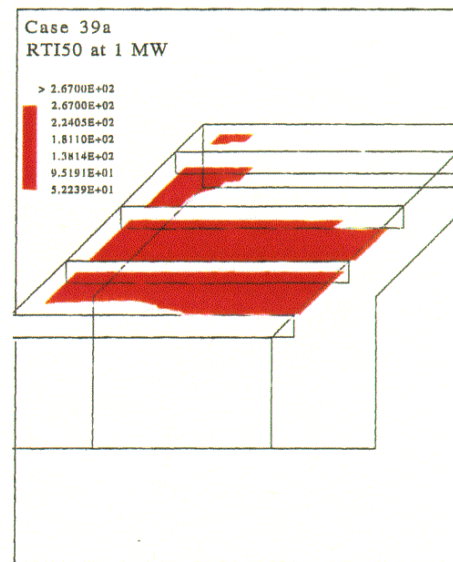
(d) 1 MW, adiabatic

Figure 11: Effect of the non-adiabatic assumption on **smoke** detector and **RTI 50** $(m\ s)^{1/2}$ **heat** sensor response for a **25 degree** sloped beamed ceiling with 0.46 m **(18 in) deep beams**. The beams are perpendicular to the slope of the ceiling. The plots are in a plane parallel to the ceiling 0.076 m **(3 in) below the ceiling**. The red contour indicates the sensor activation region.
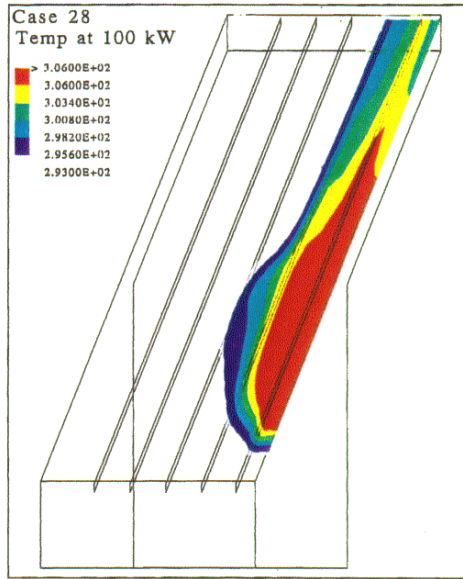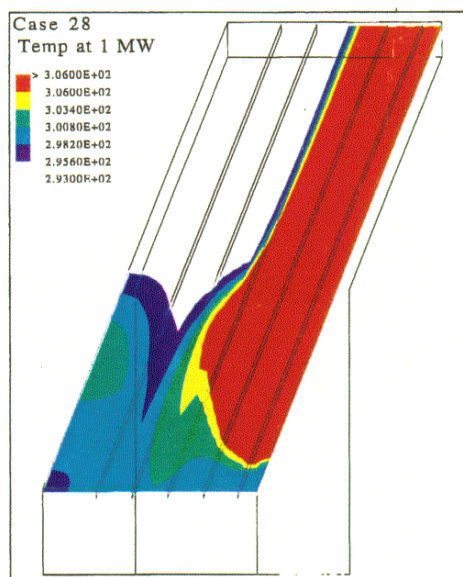
Figure 12: Contour plots illustrating the effect of gaps at the top of a beam on **smoke** detector response. Each case has a **50 degree** sloped beamed ceiling with 0.30 m **(12 in)** **deep beams**. The beams are parallel to the slope of the ceiling. The plots are in a plane parallel to the ceiling 0.076 m **(3 in) below the ceiling**. The red contour indicates the sensor activation region.
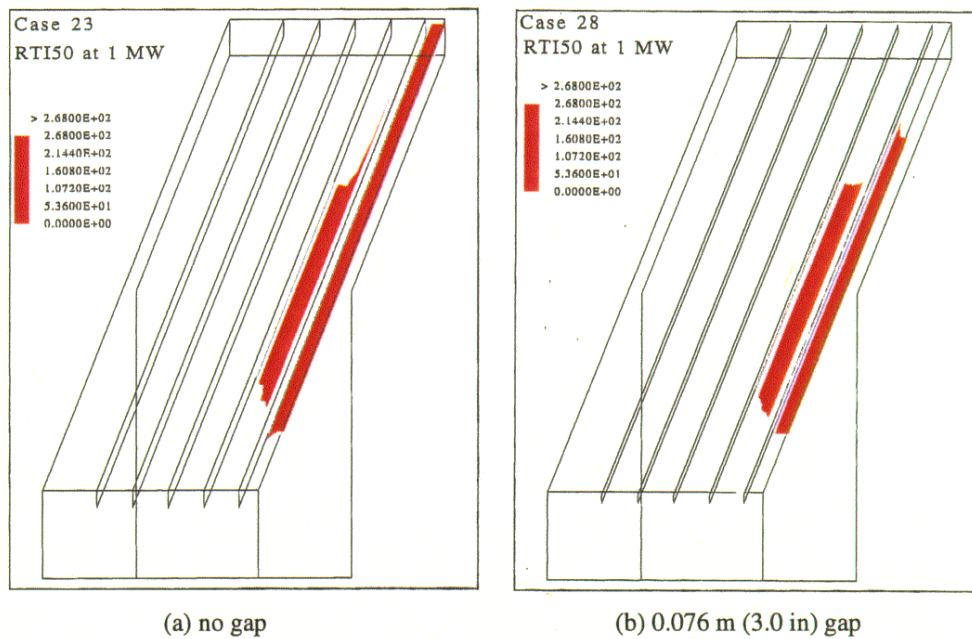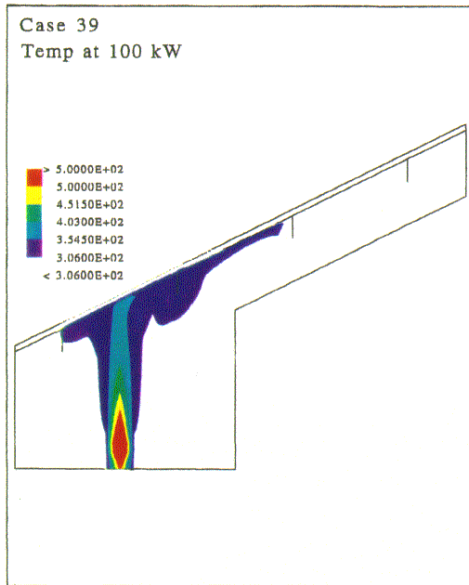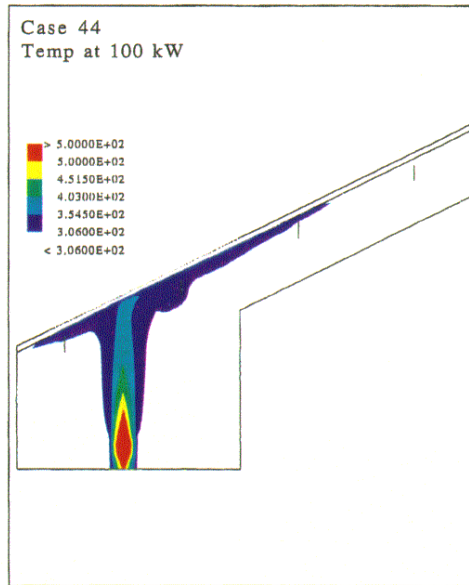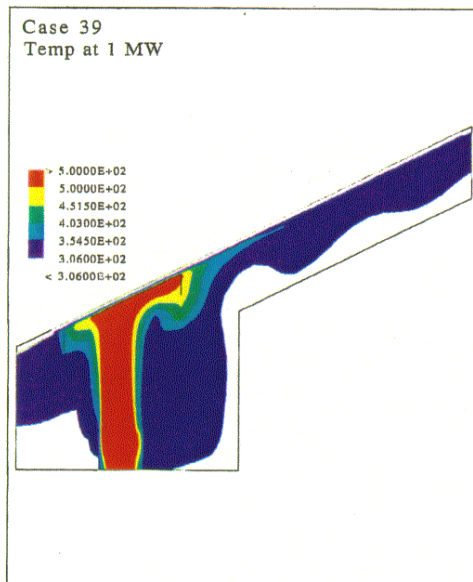
30

(a) no gap (b) 0.076 m (3.0 in) gap

Figure 13: Contour plots illustrating the effect of gaps at the top of a beam on **heat** sensor response. Both cases have a **50 degree** sloped beamed ceiling with 0.30 m **(12 in) deep beams**. The beams are parallel to the slope of the ceiling. The plot is in a plane parallel to the ceiling 0.076 m **(3 in) below the ceiling**. The red contour indicates the sensor activation region.
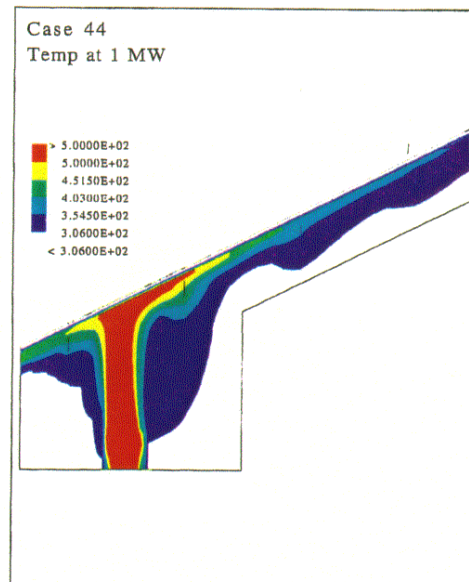
(a) 100 kW, no gap   (b) 100 kW, 0.13 m (5.0 in) gap

(c) 1 MW, no gap   (d) 1 MW, 0.13 m (5.0 in) gap

Figure 14: Contour plots illustrating the effect of gaps at the top of a beam on **smoke** detector response. Each case has a **25 degree** sloped beamed ceiling with 0.46 m (**18 in**) **deep beams**. The beams are perpendicular to the slope of the ceiling. The plots are in a vertical plane containing the fire. The Contours indicate the smoke detector activation region.
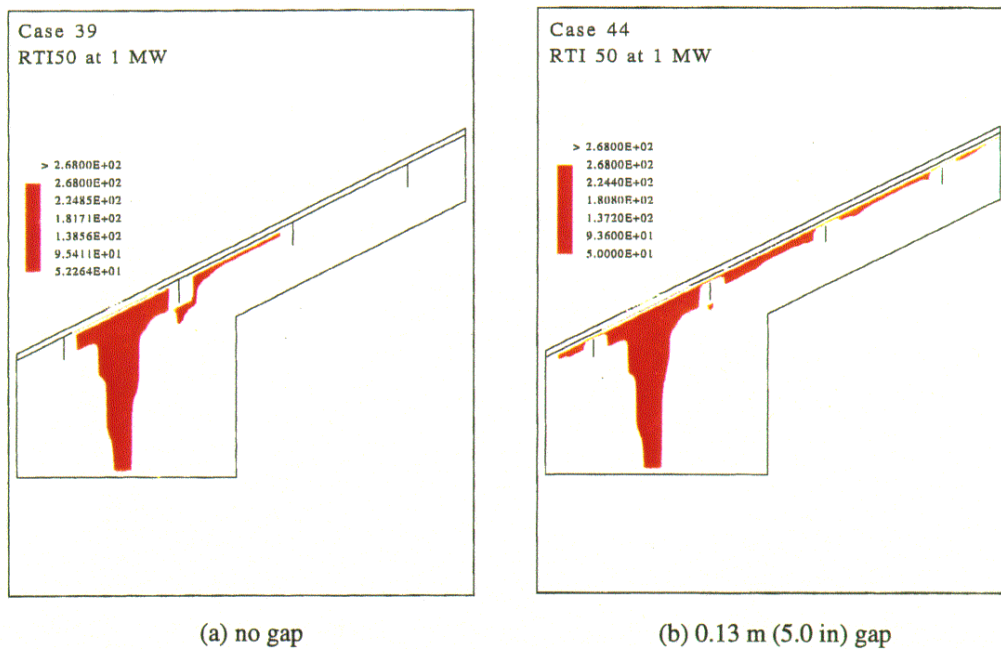
Case 39
RTI50 at 1 MW

> 2.6800E+02
2.6800E+02
2.2485E+02
1.8171E+02
1.3856E+02
9.5411E+01
5.2264E+01

Case 44
RTI 50 at 1 MW

> 2.6800E+02
2.6800E+02
2.2440E+02
1.8080E+02
1.3720E+02
9.3600E+01
5.0000E+01

(a) no gap   (b) 0.13 m (5.0 in) gap

Figure 15: Contour plots illustrating the effect of gaps at the top of a beam on **RTI 50** $(m\,s)^{1/2}$ **heat** sensor response. Each case has a **25 degree** sloped beamed ceiling with 0.46 m **(18 in) deep beams**. The beams are perpendicular to the slope of the ceiling. The plots are in a vertical plane containing the fire. The red contour indicates the sensor activation region.

33
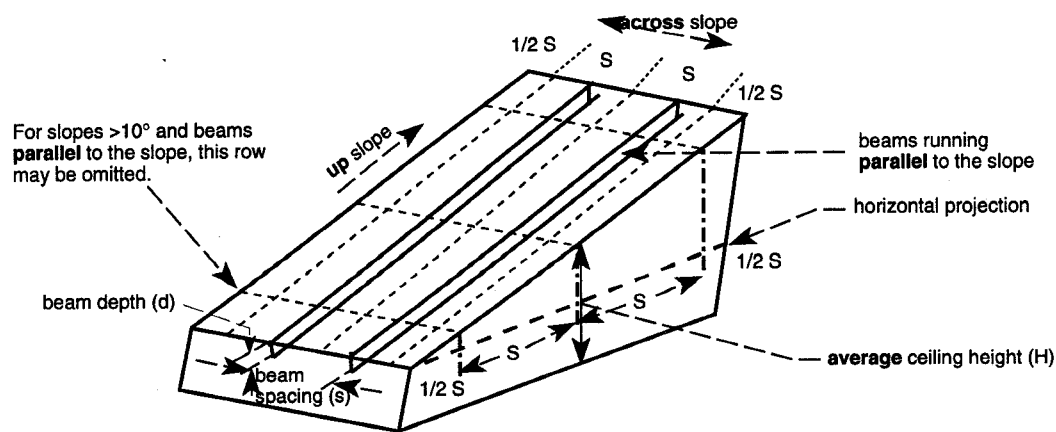
For smoke detectors and Q_d=100kW;
Spacing is S up slope and 1/2 S across slope. For
H=12' or less and d=1' or less, detectors may be
on bottom of beams or ceiling. For H exceeding
12' or d exceeding 1', ceiling mount only.
Where beams run **perpendicular** to (across) the
slope, spacing is S across slope and 1/2 S up slope.

For smoke detectors and Q_d=1MW;
Where slope is 10° or less, spacing is S up slope and 1/2
S across slope. Where slope exceeds 10°, spacing is 2S
up slope and 1/2 S across slope, detectors on bottom of
beams or ceiling. Where beams run perpendicular to the
slope,spacing is S across slope and 1/2 S up slope.

For heat detectors and Q_d=1MW;
For RTI=100 or less, and slope=10° or less, spacing is S up slope and 1/2 S
across slope. For RTI>100 or slope>10°, spacing is S up slope with detectors in
every beam channel or on the bottom of every beam. Where beams run
perpendicular to the slope and RTI is 100 or less, slope is 25° or less, **and** d is 1'
or less, spacing is S across slope and 1/2 S up slope. For RTI>100, slope>10°,
or d>1', spacing is S across slope with detectors in every beam channel or on the
bottom of every beam.

Figure 16: Schematic diagram of sloped ceiling enclosure with various spatial terminology
illustrated and spacing recommendations given.